

## Supplementary data

### Model details

#### Basic equations

The deformation process is modelled by numerical integration of the fully coupled system of 2-D conservation equations for momentum (Eq. 1), mass (Eq. 2) and energy (Eq. 3). These equations are solved together with rheological relations (Eq. 4-5) including those for a Maxwell visco-elastic body with temperature and stress dependent viscosity (Eq. 4), and a Mohr-Coulomb failure criterion with non-associated (zero dilation angle) shear flow potential (Eq. 5). It is assumed that viscous deformation consists of competing dislocation, diffusion and Peierls creep mechanisms (Kameyama et al., 1999).

$$-\frac{\partial p}{\partial x_i} + \frac{\partial \tau_{ij}}{\partial x_j} + \rho g_i = 0, \quad i = 1, 2, \quad (1)$$

$$\frac{1}{K} \frac{dp}{dt} - \alpha \frac{dT}{dt} = -\frac{\partial v_i}{\partial x_i}, \quad (2)$$

$$\rho C_p \frac{dT}{dt} = \frac{\partial}{\partial x_i} (\lambda(x_i, T) \frac{\partial T}{\partial x_i}) + \tau_{ij} \dot{\epsilon}_{ij} + \rho A \quad (3)$$

$$\frac{1}{2G} \frac{d\tau_{ij}}{dt} + \frac{1}{2\eta} \tau_{ij} = \dot{\epsilon}_{ij}; \quad \frac{1}{\eta(\tau, T)} = \frac{1}{\eta_{dif}(T)} + \frac{1}{\eta_{dis}(\tau, T)} + \frac{1}{\eta_p(\tau, T)} \quad (4)$$

$$\sigma_1 - \sigma_3 \frac{1 + \sin \phi}{1 - \sin \phi} + 2c \sqrt{\frac{1 + \sin \phi}{1 - \sin \phi}} = 0; \quad g_s = \sigma_1 - \sigma_3 \quad (5)$$

Here the Einstein summation convention applies and  $x_i$  are coordinates,  $t$  – time,  $v_i$  – velocities,  $p$  – pressure,  $\tau_{ij}$  and  $\epsilon_{ij}$  – stress and strain deviators,  $\frac{d}{dt}$  – convective time derivative,  $\frac{d\tau_{ij}}{dt}$  – Jaumann co-rotational deviatoric stress rate,  $\rho$  – density,  $g_i$  – gravity vector,  $K$  and  $G$  – bulk and shear moduli,  $\eta$  – viscosity,  $\eta_{dif}$  – diffusion creep viscosity,  $\eta_{dis}$  – dislocation creep viscosity,  $\eta_{dif}$  – Peierls creep viscosity,  $\tau$  – square root of second invariant of stress tensor,  $R$  – gas constant,  $T$  – temperature,  $\sigma_1, \sigma_3$  – maximal and minimal principal stresses,  $\phi$  – angle of friction,  $c$  – cohesion,  $C_p$  – heat capacity,  $\lambda$  – heat conductivity,  $A$  – radioactive heat production. Dependencies of all creep mechanisms viscosities from temperature and stress in (Eq.4) are taken from (Kameyama et al., 1999), with original (non-asymptotic) form of the Peierls creep viscosity. Material parameters are listed in Table RD1.

#### Interplate interface

The interface between the slab and the upper plate is modeled as a 12 km thick (3 finite elements, 2 elements at oceanic slab side and 1 element at continental plate side) subduction channel with plastic rheology. The yield stress is defined as the smallest from (Mohr-Coulomb) frictional stress:

$$\tau = c + \mu \sigma_n, \quad (6)$$

and temperature-dependent viscous shear stress (Peacock, 1996):

$$\tau = \tau_0 \exp(-(T - T_0)/\Delta T). \quad (7)$$

In (6,7),  $\tau$  is the square root of the second invariant of the stress tensor,  $c$  is cohesion,  $\sigma_n$  is normal stress,  $\mu$  is the subduction channel friction coefficient,  $T$  and  $T_0$  are local and reference temperatures,  $\tau_0$  and  $\Delta T$  are parameters. Parameters of (Eq.7),  $T_0$ ,  $\Delta T$  and  $\tau_0$ , are assumed to be 400°C, 75°C and 60 MPa, respectively, close to (Peacock, 1996).

#### Gabbro-eclogite transformation

For simplicity the same gabbro-eclogite phase diagram for the oceanic crust and continental lower crust is used, calculated for the average gabbroic composition using free Gibbs energy minimization technique (Sobolev and Babeyko, 1994). Density of the eclogite (at room conditions) is 3450 kg/m<sup>3</sup>. In all models kinetic blocking temperature for the gabbro-eclogite transformation is 800°C for the oceanic crust and 700°C for the lower continental crust.

**Table DR1.** Material parameters.

Parameter	Sediments	Felsic crust	Gabbro continent/ocean	Mantle lith-re of slab and shield	Mantle lith-re/asth-re
Density, $\rho$ , [kg/m <sup>3</sup> ]**	2670	2800	3000	3280	3280/3300
Thermal expansion, $\alpha$ , [K <sup>-1</sup> ]**	$3.7 \cdot 10^{-5}$	$3.7 \cdot 10^{-5}$	$2.7 \cdot 10^{-5}$	$3.0 \cdot 10^{-5}$	$3.0 \cdot 10^{-5}$
Elastic moduli, K, G, [GPa]**	55, 36	55, 36	63, 40	122, 74	122, 74
Heat capacity, $C_p$ , [J/kg/K]**	1200	1200	1200	1200	1200
Heat conductivity, $\lambda$ , [W/K/m]	2.5	2.5	2.5	3.3	3.3
Heat productivity, A, [ $\mu$ W/m <sup>3</sup> ]	1.3	1.3*	0.2	0	0
Initial friction angle, $\phi$ , [degree]	30	30	30	30	30
Initial cohesion, $C_h$ , [MPa]	2	20	40	40	40
Diffusion creep, $\log(A)$ , [Pa <sup>-n</sup> s <sup>-1</sup> ]	-	-	-	-10.59	-10.59
Diffusion creep activation energy, [kJ/mol]	-	-	-	300	300
Grain size[mm]_Grain size exponent	-	-	-	0.1_2.5	0.1_2.5
Dislocation creep, $\log(A)$ , [Pa <sup>-n</sup> s <sup>-1</sup> ]	-28.0	-28.0	-15.4/-25.9	-16.3	-14.3
Dislocation creep activation energy, [kJ/mol]	223	223	356/485	535	515
Power law exponent, n	4.0	4.0	3.0/4.7	3.5	3.5
Peierls creep, $\log(A)$ , [Pa <sup>-n</sup> s <sup>-1</sup> ]	-	-	-	8.5	8.5
Peierls stress, $\sigma_p$ , [GPa]	-	-	-	8.5	8.5
Peierls creep activation energy, [kJ/mol]	223	223	445	535	535

\* (Lukassen et al., 2001), \*\* (Sobolev and Babeyko, 1994)

Sources for dislocation creep laws: sediments and felsic crust – weakened (A increased by 10 times) quartzite by Gleason and Tullis (1995); mafic crust of continent – wet plagioclase by Rybacki and Dresen (2000); mafic crust of ocean – dry Columbian basalt by Mackwell et al. (1998); mantle lithosphere of slab and shield– dry peridotite by Hirth and Kohlstedt (1996), mantle lithosphere of South America (except shield) and asthenosphere – dry peridotite by Hirth and Kohlstedt (1996). Source for diffusion and Peierls creep lows in mantle- Kameyama (1999)

#### *Strain softening*

For felsic and mafic crust continental crust we assume that cohesion and friction angles linearly decrease by factor of 3 when accumulated plastic strain changes from 1 to 2. For sediments the softening is assumed to be faster; by factor 10 when accumulated plastic strain changes from 0 to 0.5. Viscosity of all continental crustal materials is assumed to decrease by factor 10 (log linearly) at finite strain 0.5-1.0.

#### **References**

- Gleason, G. C., and Tullis, J., 1995. A flow law for dislocation creep of quartz aggregates determined with the molten salt cell: Tectonophysics, v. 247, p. 1-23.
- Hirth, G., and Kohlstedt, D.L., 1996, Water in the oceanic upper mantle: implications for rheology, melt extraction and the evolution of the lithosphere: Earth Planet. Sci. Lett., v. 144, p. 93-108.
- Lucassen, F., R. Becchio, R. Harmon, S. Kasemann, G. Franz, R. Trumbull, R.L. Romer and P. Dulski, 2001. Composition and density model of the continental crust in an active continental margin – the Central Andes between 18° and 27°S, Tectonophysics 341, 195-223.
- Kameyama, M, D. A.Yuen and S.-I. Karato, 1999, Thermal-mechanical effects of low-temperature plasticity (the Peierls mechanism) on the deformation of a viscoelastic shear zone, Earth Planet. Sci. Lett. 168, 159–172.
- Mackwell, S. J., Zimmerman, M.E. & Kohlstedt, D.L. High-temperature deformation of dry diabase with application to tectonics on Venus. J. Geophys. Res. 103, 975-984 (1998).
- Rybacki, E., and G. Dresen, 2000. Dislocation and diffusion creep of synthetic anorthite aggregates, J. Geophys. Res., 105, 26017-26036.
- Sobolev, S.V. and Babeyko, A.Yu., 1994. Modeling of mineralogical composition, density and elastic wave velocities in anhydrous magmatic rocks, Surveys in Geophysics 15, 515-544.

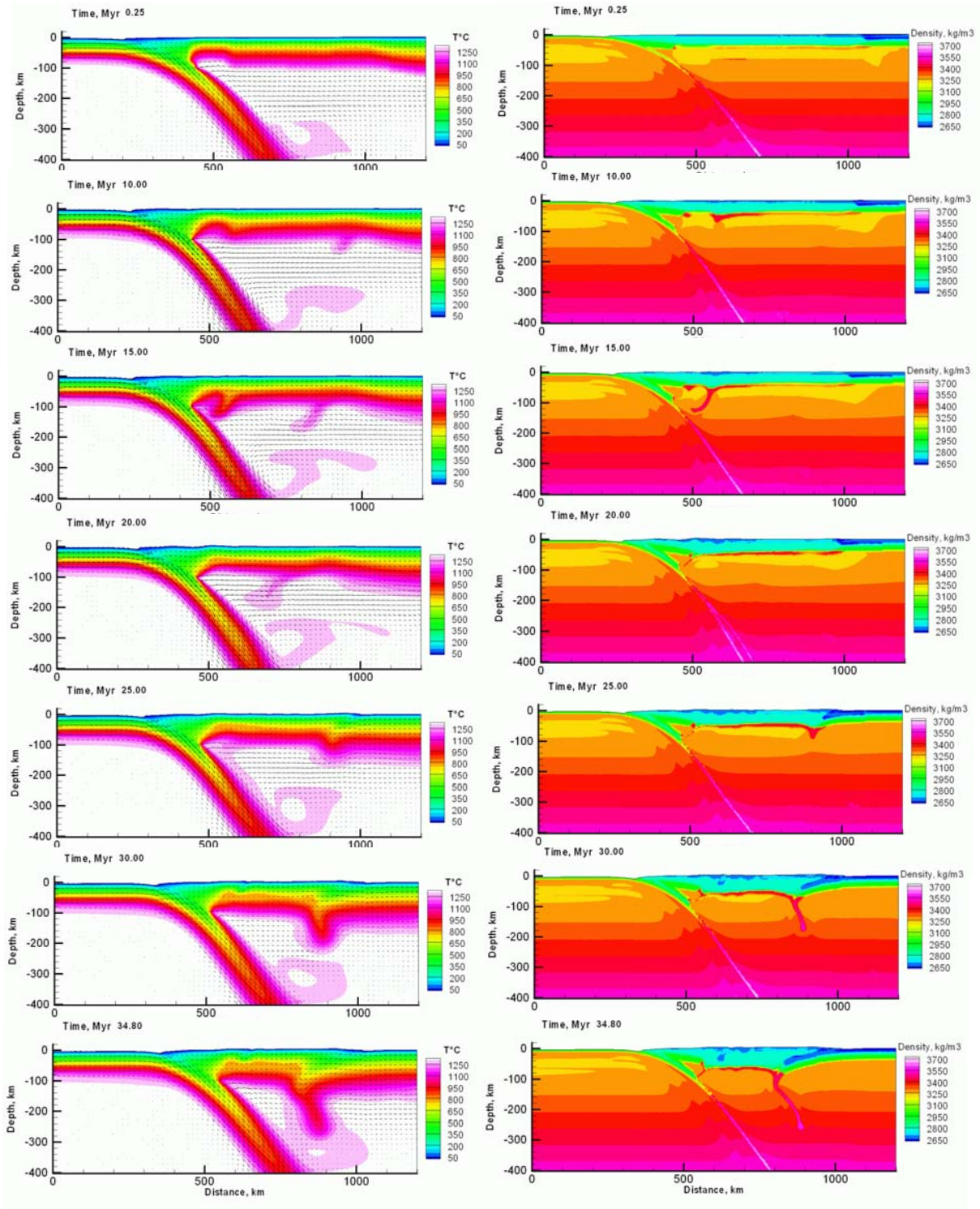


**Fig. DR1.** Time snapshots of the temperature (left) and density (right) distributions for the Central Andes model